



Remarkable catalytic activity of polymeric membranes containing gel-trapped palladium nanoparticles for hydrogenation reactions

Melissa López-Viveros^{a,*}, Isabelle Favier^b, Montserrat Gómez^b, Jean-François Lahitte^a, Jean-Christophe Remigy^{a,*}

^a Laboratoire de Génie Chimique, Université de Toulouse, CNRS, INPT, UPS, Toulouse, France

^b Laboratoire Hétérochimie Fondamentale et Appliquée, UMR CNRS 5069, Université de Toulouse 3 – Paul Sabatier, 118 route de Narbonne, 31062, Toulouse Cedex 9, France

ARTICLE INFO

Keywords:

Catalytic membrane
Palladium nanoparticles
Hydrogenations
Flat sheet membranes
Hollow fiber contactor

ABSTRACT

Polymeric flat-sheet membranes and hollow fibers were prepared via UV photo-initiated polymerization of acrylic acid at the surface of commercial polyether sulfones (PES) membranes. These polymeric materials permitted to immobilize efficiently palladium nanoparticles (PdNP), which exhibited a mean diameter in the range of 4–6 nm. These materials were synthesized by chemical reduction of Pd(II) precursors in the presence of the corresponding support. We successfully applied the as-prepared catalytic materials in hydrogenation reactions under continuous flow conditions. Flat sheet membranes were more active than hollow fibers due to the flow configuration and defavorable operating conditions. Actually, various functional groups (*i.e.* C=C, C≡C and NO₂) were reduced in flow-through configuration, under mild conditions (between 1.4 and 2.2 bar H₂ at 60 °C, using 3.2 mol% of Pd loading), archiving high conversions in short reaction times (12–24 s).

1. Introduction

Palladium is the metal of preference for many catalyzed organic reactions, due to its ability in promoting a wide range of transformations (C–halide and C–H bond activations, carbonylations (CO activation), hydrogenations (H₂ activation), *etc.*) [1]. This versatile reactivity is mainly attributed to the palladium ability for making different types of well-defined metallic species: molecular complexes, small clusters, nanoparticles, and extended surfaces [2,3]. Thus, appropriate tuning on the nature of ligands or stabilizers, and reaction conditions, leads to structures at molecular and nanometric scale [4]. Furthermore, supported palladium catalysts have been largely studied and efficiently applied for synthesis of both fine [5] and bulk chemicals [6]. Especially, working under continuous flow conditions represents a sustainable tool in terms of safety, diminution of reaction time, process intensification and scale-up [7,8]. In this frame, polymeric catalytic membranes have proven to be outstanding tools for catalytic reactions in the fine chemical industry, generally working under mild conditions (< 150 °C) [9–12]. Efficient catalytic membranes containing metal nanoparticles (MNP) have been reported for different reactions, mainly involving noble metals such as Pd, Au and Ag (C–C coupling reactions [13,14], hydrogenation of nitrates in water [15–17], hydrogenation of

unsaturated organic compounds [18–27] including the reduction of 4-nitrophenol [28–32], among others). In polymeric catalytic membranes, the catalyst can be incorporated in all the membrane (during or after its synthesis) or in a grafted polymeric layer at the surface of the membrane which stabilized the MNP by steric or electro-steric effect. This membrane modification is carried out by photo-polymerization in order to obtain polymer chains covalently linked to the membrane surface. The use of a cross linker during this step permits to control the porosity and swelling properties of the layer, leading to a polymeric gel. MNP can be prepared *via* an *ex-situ* or *in-situ* method. The *in-situ* method is based in two steps, an impregnation of the grafted layer by a metallic salt solution following by a reduction step. This last strategy is used in this work permitting the use of commercially available membranes, leading to a high experiment repeatability and high local MNP concentration at the membrane surface without aggregation. This high local concentration is the key aspect to obtain high conversions and the most relevant advantage comparing to other catalytic supports [33]. As they can be produced as either flat sheet or hollow fiber membranes, high production capacity in the order of hundred or thousand ton/year/m³ are achievable, in particular with hollow fiber membrane module [28].

Regarding the possible configurations for catalytic membrane

* Corresponding authors.

E-mail addresses: melilopezv@gmail.com (M. López-Viveros), remigy@chimie.ups-tlse.fr (J.-C. Remigy).

<https://doi.org/10.1016/j.cattod.2020.04.027>

Received 1 October 2019; Received in revised form 17 March 2020; Accepted 6 April 2020

0920-5861/ © 2020 Elsevier B.V. All rights reserved.

reactors, an important increase of the catalytic efficiency of the membranes has been already achieved before by our group when using membranes in forced flow-through configuration for the Suzuki-Miyaura C–C cross-coupling reaction compared to batch configuration under the same conditions [33,34]. Thus, we aim presenting here the results obtained in hydrogenation reactions using polymeric catalytic membranes, which contain immobilized PdNP, under a forced flow-through configuration. Moreover, we report innovative results on the hydrogenation of nitroarenes using a polymeric hollow-fiber contactor.

2. Materials and methods

2.1. Materials

Microfiltration PES flat sheet membranes MicroPES® were purchased from Membrana-3M (Wuppertal, Germany) with a nominal pore size of 0.2 µm. Microfiltration MicroPES® hollow fibers were purchased from Membrana-3M (Wuppertal, Germany), nominal pore size of 0.2 µm, inner diameter of 300 ± 40 µm and wall thickness of 100 ± 25 µm. All chemical reagents were obtained from Sigma-Aldrich and used without further purification.

2.2. Methods

2.2.1. Membrane surface modification

Surface of flat sheet PES membranes (12.4 cm^2) was functionalized by UV photo-grafting radical polymerization using a Heraeus TQ 150 lamp with a quartz filter. Membranes were dipped into monomer solutions containing 5 wt% of acrylic acid as monomer and 1.5 wt% of diethylene-di-acrylate as crosslinker (0.1 mol crosslinker /mol of monomer) and then irradiated for 3 min (total energy dose received 6.3 J cm^{-2}).

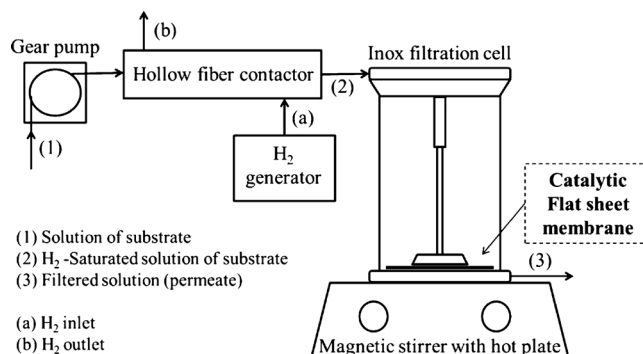
Surface of hollow PES membranes was functionalized by UV photo-grafting radical polymerization as previously described [35,36] using two high power Mercury lamps, UVA-PRINT LE, Hoenle UV France, with a line rate of 10 m min^{-1} and an intensity of the lamps of 110 % (total energy dose received 21.3 J cm^{-2}). Monomer solutions containing 20 wt% of acrylic acid as monomer and 0.85 wt% of *N,N'*-methylenebis (acrylamide) as crosslinker (0.027 mol crosslinker /mol of monomer). The change on the cross-linker was simply due to follow a previously established protocol for hollow fibers. Although both cross-linkers have different nature, the polymer gel grafted on the membrane presented the same swelling behavior in water and ethanol (probably due to similar short distances between C = C, for diethylene-diacylate: the C = C to C = C distance is 1.012 nm; for bisacrylamide, the C = C to C = C distance is 0.859 nm, according to molview modelling).

To evaluate the functionalization of the grafted membranes, ATR-FTIR was performed using a Thermo-Nicolet Nexus 670 spectrophotometer in the region of 400 to 4000 cm^{-1} and SEM images were obtained with Tabletop Microscope Phenom XL after cryofracturation.

2.2.2. In-situ synthesis of palladium nanoparticles and their characterization

The synthesis of PdNP was carried out based on the intermatrix method [37]. Grafted membranes were immersed at room temperature in a 0.02 M aqueous solution of $[\text{Pd}(\text{NH}_3)_4]\text{Cl}_2$, H_2O for 18 h. PdNP were then formed by reduction of Pd(II) ions through immersion of the membrane in a 0.1 M aqueous solution of NaBH_4 for 1 h. Membranes were thoroughly washed (30 ml of ethanol for 1 h each time) and stocked in ethanol before use.

Palladium content was determined by Inductively Coupled Plasma Optical Emission Spectrometry analyses (ICP-OES, Ultima 2, Horoba Jobin Yvon). The ICP-OES detection limit for palladium is 3 ppb. Palladium loading is expressed as µg of Pd per cm^2 ; for flat sheet membranes, the mean value was obtained for at least 3 membrane samples of 1 cm^2 of surface; for hollow fibers, the mean value was obtained for at least 3 membrane samples of 2 cm length.



Scheme 1. Experimental set-up for continuous flow hydrogenation reactions using flat sheet membranes in flow-through configuration.

For PdNP characterization, grafted membrane samples were first embedded in resin and then thin slices (80 nm) were cut with a microtome. Micrographs of PdNP were obtained by Transmission Electron Microscopy (TEM, JEOL Jem 1400). For each membrane, at least 10 slices were analyzed. Size distribution of PdNP were determined using Image J software [38].

2.2.3. Catalytic experiments

2.2.3.1. Continuous flow hydrogenations using catalytic flat-sheet membranes. Reactions were carried out in flow-through configuration with the as-prepared catalytic flat sheet membranes. Solutions containing the substrate were pre-saturated with H_2 using a hollow-fiber contactor. The Gas/Liquid hollow-fiber contactor was designed to assure H_2 saturation of solutions [39].

The experimental set-up developed to perform the hydrogenation reactions in continuous mode is presented in Scheme 1.

A home-made stainless-steel filtration cell, equipped with a magnetic stir bar, was placed on a hot-plate at 65°C . The flow rate of ethanol solution containing the substrate was controlled by a gear pump (Scheme 1, (1)). The solution was sent into a home-made hollow fiber contactor module in counter-current to saturate the solution with H_2 using a hydrogen generator (Schmidlin-FDBS). The home-made hollow fiber contactor module contained 15 fibers, an effective length of 0.3 m and $4.0 \cdot 10^{-3}$ m of diameter. The H_2 saturated solution (Scheme 1, (2)) went into the filtration cell where it flowed through the membrane. 25 ml of permeate were taken for further analyses after attaining steady-state (established when passing 4 times the total dead volume: reactor volume + connection pipes volume, ca. $4 \times 85 \text{ mL}$).

The reaction time is expressed as the residence time τ of the reactant inside the membrane using the following equation:

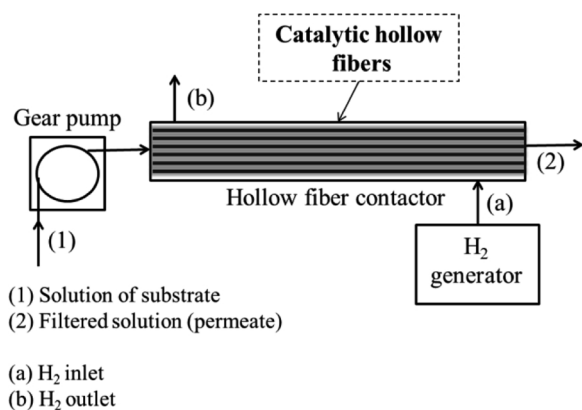
$$\tau = \frac{L}{F} \cdot \varepsilon \cdot S \quad (1)$$

with L as the membrane thickness ($110 \cdot 10^{-4} \text{ cm}$), F the permeate flow rate (mL s^{-1}) and S the membrane surface area (12.4 cm^2). The membrane porosity ε was taken as 0.8 [40].

If only the grafted layer of thickness l , where the palladium nanoparticles are found, is taken into account for the calculation, the residence time is defined as:

$$\tau^* = \frac{l}{F} \cdot \varepsilon \cdot S \quad (2)$$

Permeates (Scheme 1, (3)) were analyzed by gas chromatography (GC) using an Agilent GC6890 instrument with a flame ionization detector (FID), coupled to a Perkin Elmer Clarus MS56 mass spectrometer (MS), with a SGE BPX5 column composed by 5% of phenylmethylsiloxane and by ^1H NMR using a Bruker Avance-III 300 (300 MHz) spectrometer. Decane was used as internal standard. The palladium content in the filtered solutions and purified product was determined by ICP-OES.



Scheme 2. Experimental set-up for the continuous flow hydrogenation reactions using a catalytic hollow fiber contactor.

2.2.3.2. Continuous flow hydrogenations using G/L catalytic hollow fiber membrane contactor. The flow of the solution containing the substrate was controlled by a gear pump (Scheme 2, (1)) and sent it to the homemade G/L catalytic hollow fiber contactor module where the reaction takes place. Reaction solutions passed in the outer side of the hollow fibers while the H₂ produced by the hydrogen generator (Schmidlin-FDBS) passed in the inner side of the hollow fibers. Reactions were performed at room temperature. 15 ml of permeate (Scheme 2, (2)) were taken for further analyses after attaining steady-state (established when passing 4 times the total dead volume: reactor volume + connection pipes volume, ca. 4×5 ml).

For the G/L catalytic hollow fiber contactor, the reaction time is expressed as the residence time $\tau_{G/L}$ of the solution inside the membrane using the following equation:

$$\tau_{G/L} = \frac{V_{Cont}}{Q_l} = \frac{\pi L_{cont} [r_{cont}^2 - n_{fib} r_e^2]}{Q_l} \quad (3)$$

Where V_{Cont} is the volume of the contactor shell side (m³), Q_l the volumetric flow rate of the liquid phase (m³·s⁻¹), L_{cont} the length of the module (0.1 m), r_{cont} is the radius of the module (0.002 m), n_{fib} the number of fibers (8), r_e the external diameter of fibers (3.0·10⁻⁴ m).

Products were analyzed as described in Section 2.2.3.1.

2.2.3.3. Catalytic hydrogenations under batch configuration. Reactions were carried on in a Top Industrie autoclave. The catalytic membrane was maintained on a glass support. The substrate (0.25 mmol) was dissolved in 25 ml of ethanol. Then, the reactor was purged with argon and pressurized with H₂ (20 bar), heated at 60 °C in an oil bath and magnetically stirred for 16 h. Products were analyzed as described in Section 2.2.3.1.

3. Results and discussion

3.1. Membrane surface modification

ATR-FTIR analyses permitted to elucidate the functional groups of the PES-based membranes after photo-grafting polymerization of acrylic acid. In Fig. 1, the spectra of the flat-sheet membranes before and after photo-polymerization are presented.

The most representative bands of the PES membrane were 1578 cm⁻¹ and 1486 cm⁻¹ which correspond to C=C bond stretching of the aromatic groups of PES membrane [41]. Other characteristic absorption bands attributed to SO₂ (i.e. asymmetric and symmetric stretching, 1300 and 1150 cm⁻¹ respectively) were also observed. The analysis performed on the modified membrane showed an absorption band at 1740 cm⁻¹ attributed to the C=O vibration of the carboxylic acid group of polyacrylic acid (PAA). A broad peak below 2100 cm⁻¹

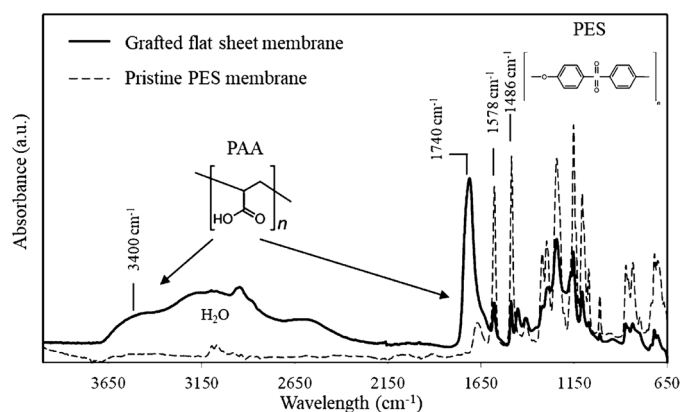


Fig. 1. ATR-FTIR spectra of grafted (—) and pristine (—) MicroPES® flat sheet membranes.

corresponds to the asymmetric O–H stretching for the modified membrane, attributed to both PAA and water trapped into the highly hydrophilic PAA layer. Spectrum of the grafted hollow fiber membrane exhibited the same absorption bands that the flat-sheet grafted membrane (see Fig. S1 in the Supplementary Information), pointing to the same type of functionalization.

Membranes were also analyzed by SEM to estimate the thickness of the grafted layers, thus corroborating the surface functionalization of the pristine membrane. Actually, SEM images of the cross-section of the modified membrane clearly showed a grafted PAA layer at the membrane surface for both flat sheets and hollow fibers (Fig. 2).

It could be observed that both membrane supports (flat sheet and hollow fiber) show highly porous structures. For the flat sheet membrane (Fig. 2a), the mean thickness of the PAA grafted layer was estimated to be ca. 3.1 μm and for the hollow fiber membrane (Fig. 2b), ca. 5.6 μm.

3.2. In-situ synthesis of palladium nanoparticles and their characterization

The PAA grafted gels on both supports, flat sheets and hollow fibers, swelled by aqueous solutions, offered a large space between crosslinked network which served for nucleation and further growth of PdNP

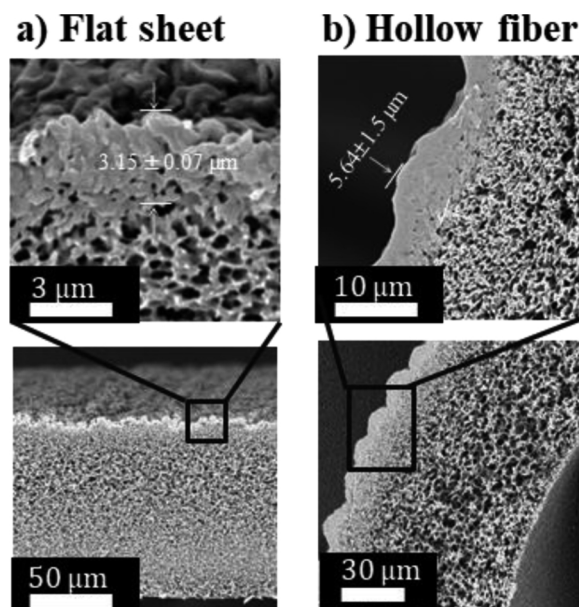


Fig. 2. SEM cross-section micrographs of: a) functionalized flat-sheet membrane and b) functionalized hollow fibers.

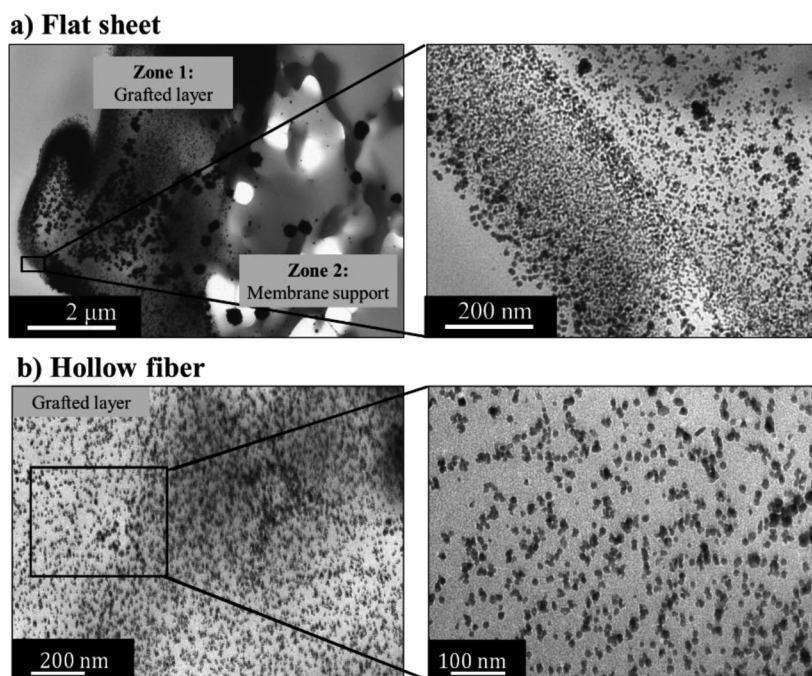


Fig. 3. TEM micrographs of PdNP in the grafted PAA layer on a) Flat sheet membrane and b) hollow fiber.

[[42]]. The *in-situ* synthesis of PdNP within the PAA was carried out in aqueous medium by the treatment of the metal precursor [Pd(NH₃)₄]Cl₂ followed by the addition of the reducing agent, NaBH₄ [43,44]. The as-prepared materials were characterized by TEM (Fig. 3). For both supports, flat sheet membranes and hollow fibers, the formation of PdNP was evidenced showing a good dispersion and quasi spherical shape. These PdNP are efficiently immobilized on the membranes within the PAA grafted gel.

Regarding PdNP incorporated in the grafted flat sheets (Fig. 3a), two zones could be identified: (i) Zone 1 corresponds to the grafted gel where PdNP are mostly well-dispersed with only few aggregates and (ii) Zone 2 corresponds to the membrane pores where PdNP form large aggregates. Without considering the aggregates, the mean diameter of PdNP was estimated to be of 5.5 ± 1.8 nm. Palladium loading was of $68 \mu\text{g cm}^{-2}$ (i.e. 0.008 mmol Pd in a flat sheet membrane of 12.4 cm^2).

For the hollow fibers (Fig. 3b), the mean diameter of particles was found 4.8 ± 1.4 nm. PdNP in the hollow fiber appeared more homogeneously dispersed than in the flat sheet membrane. Palladium content was $520 \mu\text{g cm}^{-2}$. The module prepared contains 8 fibers of 10 cm, and then the total amount of palladium in the hollow fiber module is 3.93 mg (i.e. 0.037 mmol Pd).

3.3. Catalytic experiments

3.3.1. Continuous flow hydrogenations using flat sheet membranes

For each reaction, a freshly prepared membrane was used. The total palladium (0.008 mmol)/substrate (0.25 mmol) ratio was 0.032 (i.e. 3.2 mol% Pd), considering the whole catalytic material. Hydrogenations in flow-through configuration were performed for substrates containing different functional groups (Table 1): C=C bond for both conjugated and non-conjugated compounds (entries 1–4), C≡C bond (entry 5) and NO₂ group (entries 6 and 7).

For the hydrogenation of alkene substrates, full conversion in 24 s was obtained for the indene hydrogenation, selectively reducing the conjugated C=C bond to the aromatic ring (entry 1), leading to a turnover frequency *ca.* three times higher than other conjugated substrates described in the literature [8]. However, for non-conjugated C=C bonds, such as 1-dodecene, lower conversion was achieved (26 %

conversion after recycling 3 times (x12 s) or 36 s of residence time; entry 2) with a low chemoselectivity, mainly obtaining isomerization products (i.e. internal alkenes), what indicates that this catalytic system selectively hydrogenate terminal but not internal C=C bonds; actually, for limonene, the hydrogenation was selective towards the reduction of the exocyclic C=C bond but with a low conversion (8% conversion for 24 s of residence time; entry 3). In agreement with this behavior, the internal C=C bond of ethyl oleate could not be reduced (entry 4). The hydrogenation of the C≡C bond of diphenyl acetylene mainly led to the semi-hydrogenation product, i.e. (Z)-stilbene (53 % conversion in 24 s with a (Z)-stilbene/1,2-diphenylethane ratio = 80/20; entry 5). This catalytic system was also efficient for the reduction of NO₂ of nitrobenzene (41 % conversion in 12 s, entry 6); but, for nitrobenzene containing an electron-withdrawing group, such as 4-nitrobenzonitrile, the activity dramatically decreased (21 % conversion, entry 7). Unfortunately, the reduction of aromatic aldehydes and ketones (such as benzaldehyde and acetophenone), and nitrile derivatives (benzonitrile) did not work under flow conditions even after recirculating the permeate, in contrast to batch configuration.

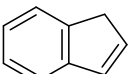
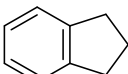
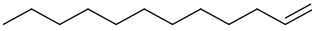
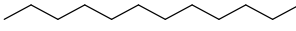
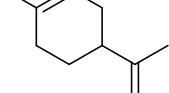
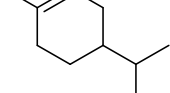
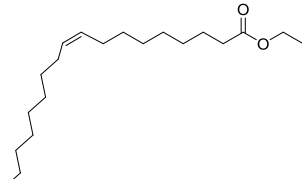
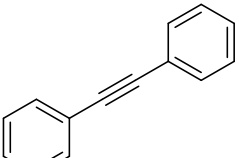
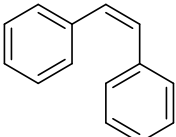
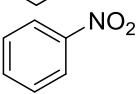
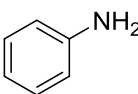
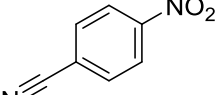
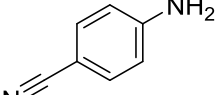
No Pd leaching was observed in any of the filtered solutions (i.e. Pd content below 3 ppb from ICP-OES analyses), which indicates that PdNP are suitably stabilized by the PAA grafted gel, permitting an efficient recycling.

With the aim of studying the effect of hydrogen pressure, hydrogenations in batch mode configuration were carried out. For this purpose, benzaldehyde, acetophenone and ethyl oleate were selected (Table 2). Reactions were performed under similar conditions than those described in flow conditions, but under 20 bar H₂ pressure for 16 h ($C_{\text{H}_2, \text{sol}} = 0.073 \text{ M}$; i.e. 10–15 times more than under flow-through configuration). In this case, conversions were calculated based on the substrate (limiting reagent).

Full hydrogenation of benzaldehyde to benzylic alcohol was achieved (entry 1, Table 2); for acetophenone, moderate conversion was obtained (46 % conversion, entry 2). However, a low conversion was attained for ethyl oleate (10 % conversion, entry 3, Table 2). These results proved the catalytic efficiency of the flat sheet membranes at high pressure. Traces of Pd were detected by ICP-OES (less than 60 ppb in the extracted organic products).

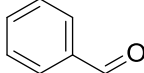
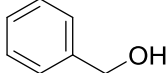
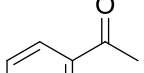
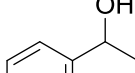
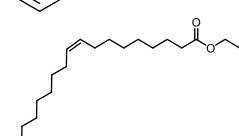
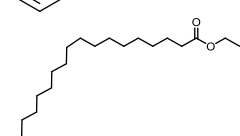
Table 1

Pd-catalyzed hydrogenation reactions in flow-through configuration in ethanol at 60 °C.

Entry	Substrate ^a	Product	P _{H2} ^b [bar] (<i>c</i> _{H2, sol} [M])	Reaction time ^c (Liquid flow rate [mL/min])	Conv. [%] (selectivity [%]) ^d [TOF (s ⁻¹)] ^g
1			1.4 (0.0051)	8 s×3 (2.0)	100 (100) [1.3]
2			2.2 (0.0080)	12 s×3 (0.8)	26 (7) ^e [0.2]
3			1.4 (0.0051)	8 s×3 (2.0)	8 (100) [0.1]
4		–	1.4 (0.0051)	8 s×3 (2.0)	0 (0)
5			2.2 (0.0080)	8 s×3 (2.0)	53 (80) ^f [0.7]
6			2.0 (0.0073)	12 s (0.8)	41 (100) [1.07]
7			2.2 (0.0080)	12 s (0.8)	21 (100) [0.55]

^a 0.25 mmol of substrate in 25 mL of ethanol (substrate concentration of 0.01 mol L⁻¹). The total palladium to substrate molar ratio was 0.032.^b H₂ absolute pressure.^c Residence time of substrates in the catalytic membrane. 8 s x 3 indicating 3 successive filtrations of 8 s each.^d Conversions were calculated based on H₂ concentration (see Supplementary Information) and determined by GC–MS and ¹H NMR using decane as internal standard.^e Main products correspond to internal alkenes formed by isomerization of the terminal C=C bond.^f In addition to (Z)-stilbene, 1,2-diphenylethane was also obtained (ca. 20 %).^g TOF = turnover frequency; TOF = conversion/(Pd load*time).**Table 2**

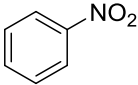
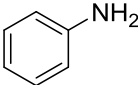
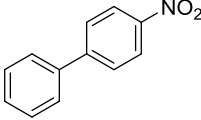
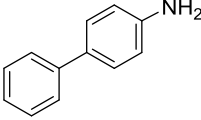
Pd-catalyzed hydrogenation reactions in batch reactor, in ethanol at 60 °C.

Entry	Substrate ^a	Product	Conversion ^b [%] (yield [%])
1			100 (100)
2			46 (46)
3			10 (100)

^a 0.25 mmol of substrate in 25 ml of ethanol (substrate concentration of 0.01 mol L⁻¹). The total palladium to substrate molar ratio was 0.032.^b Conversions and yields determined by GC–MS and ¹H NMR using decane as internal standard. Conversions were calculated based on the substrate.

Table 3

Pd-catalyzed hydrogenation reactions using a G/L catalytic hollow fiber contactor in ethanol at room temperature.

Entry	Substrate ^a	Product	P _{H2} [bar] (<i>c</i> _{H₂, sol} [M])	Reaction time (liquid flow rate [mL/min])	Conv. ^b [%] (selectivity[%]) ^c	TOF ^d (s ⁻¹)
1			1.4 (0.0051)	1.3 min (0.8)	23 (100)	0.72
2			1.4 (0.0051)	2.2 min (0.5)	22 (100)	0.41

^a 0.15 mmol of substrate in 15 ml of ethanol (substrate concentration = 0.01 mol L⁻¹). Pd/substrate = 0.246.^b Determined by GC-MS and ¹H NMR using decane as internal standard. Conversions were calculated based on the substrate.^c Selectivity towards the aniline derivative.^d TOF = turnover frequency; TOF = conversion/(Pd load*time).

As indicated in Table 1, short reaction times were required to obtain high conversions for some of the evaluated substrates (*i.e.* between 12 s and 24 s) under sustainable conditions in terms of temperature (60 °C), hydrogen pressure (1.4–2.2 bar) and solvent (ethanol). Even more, if we assume that the catalytic activity is only attributed to PdNP trapped on the PAA grafted layer, the reaction time τ^* is in fact smaller (*i.e.* τ^* between 0.34 and 0.68 s). This remarkable activity is mainly due to the high local concentration of Pd in relation to substrate (*i.e.* 120 mol of Pd per mol of substrate), while having a relatively low total Pd loading in the membrane (*i.e.* 0.008 mmol of Pd). The total palladium to substrate molar ratio was 0.032 considering the whole catalytic material.

3.3.2. Continuous flow hydrogenations using G/L catalytic hollow fibers contactor

A G/L catalytic hollow fiber contactor module was settled as a proof of concept for hydrogenation reactions. The objective was to develop simpler, more compact and efficient process by performing in the same device the hydrogenation reaction and the continuous supply of hydrogen to the catalyst surface to circumvent the low solubility of hydrogen in ethanol. The contact of the reacting phases should improve using hollow fibers in contactor mode, thanks to their high specific surface [45]. In this case, the limiting reagent is the substrate to be hydrogenated, therefore conversions were calculated based on the substrate concentration. The total palladium to substrate molar ratio was 0.246.

Encouraging results were obtained for the hydrogenation of NO₂ group using the G/L catalytic hollow fiber contactor (Table 3). Actually, the activity observed is as efficient as reported data using PdNPs immobilized on imidazolium-functionalized polymers. [46]

However, it was not possible to fairly compare catalytic performance of the G/L hollow fiber contactor (entry 1, Table 3) and the flat sheet membrane (entry 6, Table 1), since reaction conditions greatly differ and most of them are not favorable for the G/L catalytic hollow fiber (lower temperature, H₂ pressure, higher palladium content).

4. Conclusions

To sum up, new polymeric materials were prepared for the immobilization of metal nanoparticles, in this case PdNP. These as-prepared catalytic materials were applied in hydrogenations of different functional groups (NO₂, C=C, C≡C) under flow-through (flat sheet membranes) and G/L contactor (hollow fibers) configurations. For the first configuration, reactions worked under smooth conditions: low hydrogen pressure (1.4–2.2 bar) and 60 °C for short residence times (< 1 min), using relatively low Pd loading (3.2 mol%). For ketones and aldehydes, hydrogenations were not efficient in flow-through configuration, but flat sheet membranes were active under batch conditions by applying harsher conditions (20 bar H₂, 16 h). For the G/L catalytic

hollow fiber contactor, promising results were obtained for the hydrogenation of nitro-arenes.

In order to enlarge the applications scope for both flow modes, we are currently working in tuning experimental conditions (*e.g.* increasing temperature and/or residence time by decreasing liquid flow rate or increasing H₂ pressure; tuning the design of the contactor module with higher packing density).

CRediT authorship contribution statement

Melissa López-Viveros: Methodology, Investigation, Formal analysis, Conceptualization, Writing - original draft, Visualization, Writing - review & editing. **Isabelle Favier:** Methodology, Investigation, Conceptualization, Writing - review & editing. **Montserrat Gómez:** Conceptualization, Validation, Formal analysis, Writing - review & editing. **Jean-François Lahitte:** Conceptualization, Funding acquisition, Validation, Writing - review & editing. **Jean-Christophe Remigy:** Conceptualization, Formal analysis, Validation, Supervision, Funding acquisition, Writing - review & editing.

Declaration of Competing Interest

The authors declare that they have no known competing financial interests or personal relationships that could have appeared to influence the work reported in this paper.

Acknowledgements

The authors acknowledge the financial support of the French Ministry of Higher Education and Research. I. F. and M. G. thanks the Centre National de la Recherche Scientifique (CNRS) and the University Toulouse 3 - Paul Sabatier for financial support. The contribution of MSc. Mohammed-Lamine Ouinten for the development of the Python code used for the design of the G/L hollow fiber modules is also acknowledged.

Appendix A. Supplementary data

Supplementary material related to this article can be found, in the online version, at doi:<https://doi.org/10.1016/j.cattod.2020.04.027>.

References

- [1] J. Tsuji, John Wiley, S. Sons (Eds.), *Palladium Reagents and Catalysts*, John Wiley & Sons, Sussex, 2004.
- [2] B.M. Trost, *Metal Catalyzed Allylic Alkylation: Its Development in the Trost Laboratories*, *Tetrahedron* 71 (35) (2015) 5708–5733.
- [3] I. Favier, D. Madec, E. Teuma, M. Gomez, *Palladium nanoparticles applied in organic synthesis as catalytic precursors*, *Curr. Org. Chem.* 15 (18) (2011) 3127–3174.

- [4] R. Ciriminna, V. Pandarus, F. Béland, Y.-J. Xu, M. Pagliaro, Heterogeneously catalyzed alcohol oxidation for the fine chemical industry, *Org. Process Res. Dev.* 19 (11) (2015) 1554–1558.
- [5] H.-U. Blaser, A. Indolese, A. Schnyder, H. Steiner, M. Studer, Supported palladium catalysts for fine chemicals synthesis, *J. Mol. Catal. A Chem.* 173 (1–2) (2001) 3–18.
- [6] N. Pernicone, M. Cerboni, G. Prelazzi, F. Pinna, G. Fagherazzi, An investigation on Pd/C industrial catalysts for the purification of terephthalic acid, *Catal. Today* 44 (1–4) (1998) 129–135.
- [7] L. Vaccaro, D. Lanari, A. Marrocchi, G. Strappaveccia, Flow approaches towards sustainability, *Green Chem.* 16 (8) (2014) 3680–3704.
- [8] A. Reina, I. Favier, E. Teuma, M. Gómez, A. Conte, L. Pichon, Hydrogenation reactions catalyzed by colloidal palladium nanoparticles under flow regime, *AIChE J.* (2019).
- [9] I.F.J. Vankelecom, Polymeric membranes in catalytic reactors, *Chem. Rev.* 102 (2002) 3779–3810.
- [10] S.S. Ozdemir, M.G. Buonomenna, E. Drioli, Catalytic Polymeric Membranes: Preparation and Application, *Appl. Catal. A Gen.* 307 (2) (2006) 167–183.
- [11] A. Brunetti, P.F. Zito, L. Giorno, E. Drioli, G. Barbieri, Membrane reactors for low temperature applications: an overview, *Chem. Eng. Process. Process Intensif.* 124 (May 2017) (2018) 282–307.
- [12] R. Poupard, D. Grande, B. Carbonnier, B. Le Droumaguet, Porous Polymers and Metallic Nanoparticles: A Hybrid Wedding as a Robust Method toward Efficient Supported Catalytic Systems, *Prog. Polym. Sci.* 96 (2019) 21–42.
- [13] L.F. Villalobos, P. Neelakanda, M. Karunakaran, D. Cha, K.V. Peinemann, Poly-Thiosemicarbazide/Gold Nanoparticles Catalytic Membrane: In-Situ Growth of Well-Dispersed, Uniform and Stable Gold Nanoparticles in a Polymeric Membrane, *Catal. Today* 236 (2014) 92–97.
- [14] V.W. Faria, D.G.M. Oliveira, M.H.S. Kurz, F.F. Gonçalves, C.W. Scheeren, G.R. Rosa, Palladium nanoparticles supported in a polymeric membrane: an efficient phosphine-free “Green” catalyst for suzuki-miyaura reactions in water, *RSC Adv.* 4 (26) (2014) 13446–13452.
- [15] O.M. Ilinich, E.N. Gribov, P.A. Simonov, Water denitrification over catalytic membranes: hydrogen spillover and catalytic activity of macroporous membranes loaded with Pd and Cu, *Catal. Today* 82 (1–4) (2003) 49–56.
- [16] O.M. Ilinich, F.P. Cuperus, L.V. Nosova, E.N. Gribov, Catalytic Membrane in Reduction of Aqueous Nitrates: Operational Principles and Catalytic Performance, *Catal. Today* 56 (1–3) (2000) 137–145.
- [17] X. Zhu, K. Choo, J. Park, Nitrate removal from contaminated water using poly-electrolyte-enhanced ultrafiltration, *Desalination* 193 (August 2005) (2006) 350–360.
- [18] S.R. Hogg, S. Muthu, M.O. Callaghan, J. Lahitte, M.L. Bruening, Wet air oxidation of formic acid using nanoparticle-modified polysulfone hollow fibers as gas – liquid contactors, *ACS Appl. Mater. Interfaces* 4 (2012) 1440–1448.
- [19] F. Peirano, T. Vincent, F. Quignard, M. Robitzer, E. Guibal, Palladium supported on chitosan hollow Fiber for nitrotoluene hydrogenation, *J. Memb. Sci.* 329 (1–2) (2009) 30–45.
- [20] R. Van der Vaart, V.I. Lebedeva, I.V. Petrova, L.M. Plyasova, N.A. Rudina, D.I. Kochubey, G.F. Tereshchenko, V.V. Volkov, J. Van Erkel, Preparation and characterisation of palladium-loaded polypropylene porous hollow fibre membranes for hydrogenation of dissolved oxygen in water, *J. Memb. Sci.* 299 (1–2) (2007) 38–44.
- [21] C. Liu, Y. Xu, S. Liao, D. Yu, Y. Zhao, Y. Fan, Selective hydrogenation of Propadiene and propyne in Propene with catalytic polymeric hollow-fiber reactor, *J. Memb. Sci.* 137 (1–2) (1997) 139–144.
- [22] D. Singh, M.E. Rezac, P.H. Pfromm, Partial Hydrogenation of Soybean Oil Using Metal-Decorated Integral-Asymmetric Polymer Membranes: Effects of Morphology and Membrane Properties, *J. Memb. Sci.* 348 (1–2) (2010) 99–108.
- [23] L. Gröschel, R. Haidar, A. Beyer, H. Cölfen, B. Frank, R. Schomäcker, Hydrogenation of propyne in palladium-containing polyacrylic acid membranes and its characterization, *Ind. Eng. Chem. Res.* 44 (24) (2005) 9064–9070.
- [24] A. Bottino, G. Capannelli, A. Comite, R. Di Felice, Polymeric and ceramic membranes in three-phase catalytic membrane reactors for the hydrogenation of methylenecyclohexane, *Desalination* 144 (1–3) (2002) 411–416.
- [25] D. Fritsch, K. Kuhr, K. Mackenzie, F.D. Kopinke, Hydrodechlorination of Chloroorganic Compounds in Ground Water by Palladium Catalysts: Part 1. Development of Polymer-Based Catalysts and Membrane Reactor Tests, *Catal. Today* 82 (1–4) (2003) 105–118.
- [26] L. Brandão, L.M. Madeira, A.M. Mendes, Propyne hydrogenation in a continuous polymeric catalytic membrane reactor, *Chem. Eng. Sci.* 62 (23) (2007) 6768–6776.
- [27] D. Fritsch, K.V. Peinemann, Catalysis with homogeneous membranes loaded with nanoscale metallic clusters and their preparation, *Catal. Today* 25 (3–4) (1995) 277–283.
- [28] R. Hilke, N. Pradeep, P. Madhavan, U. Vainio, A.R. Behzad, R. Sougrat, S.P. Nunes, K. Peinemann, Block copolymer hollow Fiber membranes with catalytic activity and PH-Response, *Appl. Mater. Interfaces* 5 (2013) 7001–7006.
- [29] H. Wang, Z. Dong, C. Na, Hierarchical carbon nanotube membrane-supported gold nanoparticles for rapid catalytic reduction of p -Nitrophenol, *ACS Sustain. Chem. Eng.* 1 (7) (2013) 746–752.
- [30] A. Mashentseva, D. Borgekov, S. Kisilitsin, M. Zdorovets, A. Migunova, Comparative catalytic activity of PET track-etched membranes with embedded silver and gold nanotubes, *Nucl. Instruments Methods Phys. Res. Sect. B Beam Interact. Mater. Atoms* 365 (2015) 70–74.
- [31] Y. Liu, M. Li, G. Chen, A New Type of Raspberry-like Polymer Composite Sub-Microspheres with Tunable Gold Nanoparticles Coverage and Their Enhanced Catalytic Properties, *J. Mater. Chem. A* 1 (3) (2013) 930–937.
- [32] B. Doménech, M. Muñoz, D.N. Muraviev, J. Macanás, Catalytic membranes with palladium nanoparticles: from tailored polymer to catalytic applications, *Catal. Today* 193 (1) (2012) 158–164.
- [33] Y. Gu, P. Bacchin, J. Lahitte, J. Remigy, I. Favier, M. Gómez, D.L. Gin, R.D. Noble, Catalytic membrane reactor for suzuki-miyaura C – C cross-coupling: explanation for its high efficiency via modeling, *AIChE J.* 63 (2) (2017) 698–704.
- [34] Y. Gu, I. Favier, C. Pradel, D.L. Gin, J.F. Lahitte, R.D. Noble, M. Gómez, J.C. Remigy, High catalytic efficiency of palladium nanoparticles immobilized in a polymer membrane containing poly(ionic liquid) in suzuki-miyaura cross-coupling reaction, *J. Memb. Sci.* 492 (2015) 331–339.
- [35] A. Akbari, S. Desclaux, J.C. Rouch, J.C. Remigy, Application of nanofiltration hollow fibre membranes, developed by Photografting, to treatment of anionic dye solutions, *J. Memb. Sci.* 297 (1–2) (2007) 243–252.
- [36] P.T. Nguyen, E. Lasseguette, Y. Medina-gonzalez, J.C. Remigy, D. Roizard, E. Favre, A dense membrane contactor for intensified CO 2 gas / liquid absorption in post-combustion capture, *J. Memb. Sci.* 377 (1–2) (2011) 261–272.
- [37] D.N. Muraviev, J. Macanás, J. Parrondo, M. Muñoz, A. Alonso, S. Alegret, M. Ortueta, F. Mijangos, Cation-exchange membrane as nanoreactor: intermatrix synthesis of platinum-copper core-shell nanoparticles, *React. Funct. Polym.* 67 (12 SPEC. ISS) (2007) 1612–1621.
- [38] C.A. Schneider, W.S. Rasband, K.W. Eliceiri, NIH image to ImageJ: 25 years of image analysis, *Nat. Methods* 9 (2012) 7.
- [39] A. Gabelman, S.T. Hwang, Hollow Fiber membrane contactors, *J. Memb. Sci.* 159 (1–2) (1999) 61–106.
- [40] R.W. Baker, S.P. Nunes, K. Peinemann (Eds.), *Membrane Technology*, Wiley, 2006.
- [41] S. Belfer, R. Fainchtain, Y. Purinson, O. Kedem, Surface Characterization by FTIR-ATR Spectroscopy of Polyethersulfone Membranes-Unmodified, Modified and Protein Fouled, 172 (2000) 113–124.
- [42] K. Karami, M. Ghasemi, N. Haghighat Naeini, Palladium nanoparticles supported on polymer: an efficient and reusable heterogeneous catalyst for the Suzuki cross-coupling reactions and aerobic oxidation of alcohols, *Catal. Commun.* 38 (2013) 10–15.
- [43] D.B. Pacardo, M.R. Knecht, Pd Nanoparticles in C-C Coupling Reactions, (2014), pp. 112–156.
- [44] M. Kralik, A. Biffis, Catalysis by metal nanoparticles supported on functional organic polymers, *J. Mol. Catal. A Chem.* 177 (1) (2001) 113–138.
- [45] R. Dittmeyer, K. Svajda, M. Reif, A review of catalytic membrane layers for gas / liquid reactions, *Top. Catal.* 29 (May) (2004) 3–27.
- [46] S. Doherty, J.G. Knight, T. Backhouse, A. Bradford, F. Saunders, R.A. Bourne, T.W. Chamberlain, R. Stones, A. Clayton, K. Lovelock, *Catal. Sci. Technol.* 8 (5) (2018) 1454–1467.